Computational Structural Engineering
An International Journal
Vol. 1, No. 1, pp. 39~48 (2001)

Computational Structural Engineering Institute

Analytical Algorithm Predicting Compressive Stress-Strain Relationship for Concrete Confined with Laminated Carbon Fiber Sheets

Sang-Ho Lee† and Hyo-Jin Kim

Department of Civil Engineering, Yonsei University, Seoul 120-749, Korea

Received November 2000; Accepted April 2001

ABSTRACT

An analytical compressive stress-strain relationship model for circular and rectangular concrete specimens confined with laminated carbon fiber sheets (CFS) is studied. Tsai-Hill and Tsai-Wu failure criteria were used to implement orthotropic behavior of laminated composite materials. By using these criteria, an algorithm which analyzes the confinement effect of CFS on concrete was developed. The proposed analytical model was verified through the comparison with experimental data. Various parameters such as concrete strength, ply angle, laminate thickness, section shape, and ply stacking sequences were investigated. Numerical results by the proposed model effectively simulate the experimental compressive stress-strain behavior of CFS confined concrete specimens. Also, the proposed model estimates the compressive strength of the specimen to a high degree of accuracy.

Keywords: stress-strain relation, laminated carbon fiber sheets, Tsai-Hill and Tsai-Wu failure criteria, confinement effects

1. Introduction

It is inevitable that reinforced concrete structures deteriorate over time due to aging, fatigue, and other environmental factors. Recently, a quick and simple solution of rehabilitating the deteriorated concrete members by wrapping them with carbon fiber sheets (CFS) became popular, and many researches on this retrofitting method have been performed. Many experimental studies have been performed by domestic researchers to estimate the strengthening effects of compressive concrete members strengthened by CFS. For example, Lim and Chung (1992), Kwon and Chung (1999), and Lee and Koo (1999) studied the strengthening effect of confined concrete columns. Choi *et al.* (1999) and Jang *et al.* (1999) studied the stress-strain relationship, the confinement effect, and the strength enhan-cement of strengthened compressive members experimentally. In addition, a couple of empirical equations for the estimation of strengthening stresses in compressive members have been suggested (Jeong *et al.*, 1997; Lee *et al.*, 1998). The time has come to develop a fundamentally sound analytical model that can simulate the experimental results on the confinement effect of carbon fiber sheets for retrofitting of concrete members. Unfortunately, a lack of analytical researches on this topic has not solved the need for an analytical model that can represent generic properties of CFS laminate as well as concrete members in a consistent manner.

The behavior of laminated CFS wrapped concrete member in compression is governed by several parameters such as fiber alignment characteristics of CFS, the failure behavior of laminated composite materials, and the confinement effects in concrete. Popovics (1973) introduced a numerical model for the stress-strain relationship of confined concrete. Several researchers performed similar studies, analytically and experimentally, based on hoop and spiral reinforcements (Scott *et al.*, 1982; Ahmed and Shah, 1985; Priestley and Park, 1987; Mander *et al.*, 1988). Saadatmanesh *et al.* (1994) proposed a analytical model to evaluate confining effect of carbon fiber sheets which were used to retrofit bridge columns. They studied the confining effects based on P-M-ϕ curves of the columns. Empirical studies were also carried out by Hosotani *et al.* (1997, 1998). Recently,

† Corresponding author
Tel.: +82-2-2123-2808; Fax: +82-2-364-5300
E-mail address: lee@yonsei.ac.kr

Malek and Saadatmanesh (1998) applied a laminate theory to analyze shear-strengthened beam with CFS. However, the major flaw of all these studies is that they do not consider the fundamental characteristics of laminates.

In this study, an analysis is performed to obtain the stress-strain relationship of concrete member confined with laminated carbon fiber sheets in compression by implementing specific characteristics of retrofitted fiber reinforced composite.

2. Analysis on the Behavior of Laminates

2.1 Stress-strain relationship of lamina

A lamina, or ply, is a plane layer of unidirectional fibers or woven fabric in a matrix. The lamina is an orthotropic material with principal material axes in the direction of the fibers (longitudinal), normal to the fibers in the plane of the lamina (in-plane transverse), and normal to the plane of the lamina. For an orthotropic material which has three mutually perpendicular planes of material symmetry, the stress-strain relationships can be defined as

$$\begin{Bmatrix} \sigma_{11} \\ \sigma_{22} \\ \sigma_{33} \\ \tau_{23} \\ \tau_{31} \\ \tau_{12} \end{Bmatrix} = \begin{bmatrix} C_{11} & C_{12} & C_{13} & 0 & 0 & 0 \\ C_{12} & C_{22} & C_{23} & 0 & 0 & 0 \\ C_{13} & C_{23} & C_{33} & 0 & 0 & 0 \\ 0 & 0 & 0 & C_{44} & 0 & 0 \\ 0 & 0 & 0 & 0 & C_{55} & 0 \\ 0 & 0 & 0 & 0 & 0 & C_{66} \end{bmatrix} = \begin{Bmatrix} \varepsilon_{11} \\ \varepsilon_{22} \\ \varepsilon_{33} \\ \gamma_{23} \\ \gamma_{31} \\ \gamma_{12} \end{Bmatrix} \tag{1}$$

where C_{ij} are the stiffness matrix components.

In most structural applications, composite materials are used in the form of thin laminates loaded in the plane direction. Thus, a composite lamina can be assumed to have plane stress condition with all the stress components in the out-of-plane direction being zero, i.e., $\sigma_{33} = \tau_{23} = \tau_{13} = 0$. Then, the stress-strain relationships for lamina, Eq. (1) can be reduced to

$$\begin{Bmatrix} \sigma_{11} \\ \sigma_{22} \\ \sigma_{13} \end{Bmatrix} = \begin{bmatrix} Q_{11} & Q_{13} & 0 \\ Q_{12} & Q_{22} & 0 \\ 0 & 0 & Q_{66} \end{bmatrix} = \begin{Bmatrix} \varepsilon_{11} \\ \varepsilon_{22} \\ \gamma_{12} \end{Bmatrix} \tag{2}$$

vhere the reduced stiffness matrix components (Lee *et al.*, 995) are

$$Q_{ij} = C_{ij} - \frac{C_{i3}C_{j3}}{C_{33}} \qquad (i,j = 1,2,6) \tag{3}$$

the compliance matrix is represented as

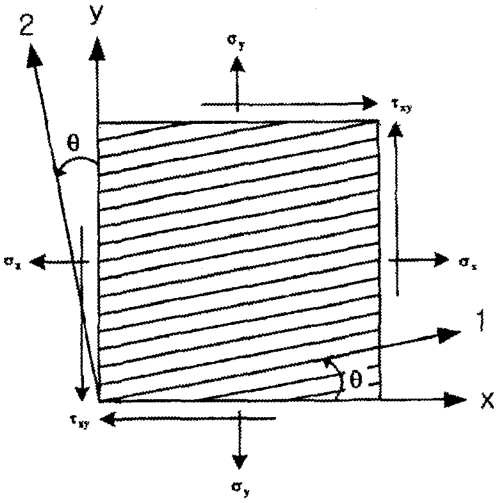

(a) on the loading axes

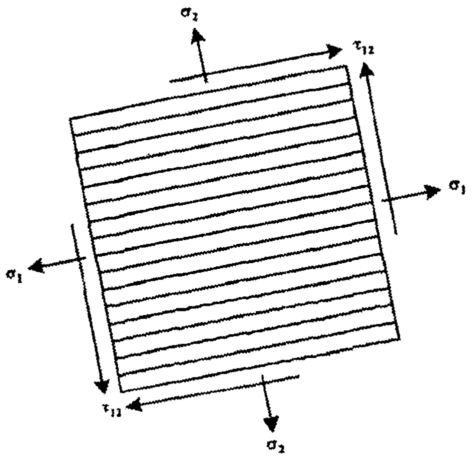

(b) on the material axes

Fig. 1. Stress components in unidirectional lamina referred tc loading and material axes.

$$\begin{Bmatrix} \varepsilon_{11} \\ \varepsilon_{22} \\ \gamma_{12} \end{Bmatrix} = \begin{bmatrix} S_{11} & S_{12} & 0 \\ S_{12} & S_{22} & 0 \\ 0 & 0 & S_{66} \end{bmatrix} = \begin{Bmatrix} \sigma_{11} \\ \sigma_{22} \\ \sigma_{12} \end{Bmatrix} \tag{4}$$

Generally, the lamina principal axes do not coincide with the loading or reference axes (Fig. 1). Then, the stress and strain components referred to the principal material axes can be expressed in terms of those referred to the loading axes by the following transformation relationships

$$\begin{bmatrix} \sigma_1 \\ \sigma_2 \\ \sigma_3 \end{bmatrix} = \begin{bmatrix} T_\sigma \end{bmatrix} \begin{bmatrix} \sigma_x \\ \sigma_y \\ \tau_{xy} \end{bmatrix} \tag{5}$$

and

$$\begin{bmatrix}\varepsilon_1\\ \varepsilon_2\\ \gamma_{12}\end{bmatrix} = \begin{bmatrix}T_g\end{bmatrix}\begin{bmatrix}\sigma_x\\ \sigma_y\\ \tau_{xy}\end{bmatrix} \quad (6)$$

where the transformation matrix $[T_\sigma]$ is given by Eq. (7) and $[T_g] = [T_\sigma]^{-T}$.

$$[T_\sigma] = \begin{bmatrix} m^2 & n^2 & 2mn \\ n^2 & m^2 & -2mn \\ -mn & mn & m^2-n^2 \end{bmatrix} \quad (7)$$

where $m = \cos\theta$, $n = \sin\theta$.

Using Eq. (5) and Eq. (6), the stress-strain relationships based on the loading axes can be expressed as

$$\begin{Bmatrix}\sigma_x\\ \sigma_y\\ \tau_s\end{Bmatrix} = [T_\sigma]^{-1}\begin{Bmatrix}\sigma_{11}\\ \sigma_{22}\\ \tau_{12}\end{Bmatrix} = [T_\sigma]^{-1}[Q][T_\varepsilon]\begin{Bmatrix}\varepsilon_x\\ \varepsilon_y\\ \gamma_s\end{Bmatrix} = [\overline{Q}]\begin{Bmatrix}\varepsilon_x\\ \varepsilon_y\\ \gamma_s\end{Bmatrix} \quad (8)$$

where $\tau_s = \tau_{xy}$ is shear stress, $\gamma_s = \gamma_{xy}$ is shear strain, and $[\overline{Q}]$ is transformed reduced stiffness matrix.

2.2 Stress-strain relationship of laminate

A laminate is made up of two or more unidirectional laminas or plies stacked together at various orientations. For a lamina, we can relate the strains at any point in the laminate to those of reference plane strains and the laminate curvatures. Consider an individual layer k in a multidirectional laminate whose mid-plane is at a distance from the laminate reference plane. The stress-strain relationships for this layer based on a laminate coordinate system is

$$\begin{Bmatrix}\sigma_x\\ \sigma_y\\ \tau_s\end{Bmatrix}_k = \begin{bmatrix}Q_{xy} & Q_{xy} & Q_{xs}\\ Q_{yx} & Q_{yy} & Q_{ys}\\ Q_{sx} & Q_{sy} & Q_{ss}\end{bmatrix}_k\begin{Bmatrix}\varepsilon_x^0\\ \varepsilon_y^0\\ \gamma_s^0\end{Bmatrix} + z\begin{bmatrix}Q_{xx} & Q_{xy} & Q_{xs}\\ Q_{xy} & Q_{yy} & Q_{ys}\\ Q_{sx} & Q_{sy} & Q_{ss}\end{bmatrix}_k\begin{Bmatrix}\kappa_s\\ \kappa_y\\ \kappa_s\end{Bmatrix} \quad (9)$$

where ε_{ij}^0 are the strain components on the reference plane, κ_{ij} are the curvatures of the laminate, and z is the distance from neutral surface defined by the reference plane. Integrating Eq. (9) along the thickness, the forces and the moments for the n-laminate plies are

$$\begin{Bmatrix}N_x\\ N_y\\ N_s\end{Bmatrix} = \begin{bmatrix}A_{xx} & A_{xy} & A_{xs}\\ A_{xy} & A_{yy} & A_{ys}\\ A_{sx} & A_{sy} & A_{ss}\end{bmatrix}\begin{Bmatrix}\varepsilon_x^0\\ \varepsilon_y^0\\ \gamma_s^0\end{Bmatrix} + \begin{bmatrix}B_{xx} & B_{xy} & B_{xs}\\ B_{yx} & B_{yy} & B_{ys}\\ B_{sx} & B_{sy} & B_{ss}\end{bmatrix}\begin{Bmatrix}\kappa_x\\ \kappa_y\\ \kappa_s\end{Bmatrix} \quad (10)$$

and

$$\begin{Bmatrix}M_x\\ M_y\\ M_s\end{Bmatrix} = \begin{bmatrix}B_{xx} & B_{xy} & B_{xs}\\ B_{yx} & B_{yy} & B_{ys}\\ B_{sx} & B_{sy} & B_{ss}\end{bmatrix}\begin{Bmatrix}\varepsilon_x^0\\ \varepsilon_y^0\\ \gamma_s^0\end{Bmatrix} + \begin{bmatrix}D_{xx} & D_{xy} & D_{xs}\\ D_{yx} & D_{yy} & D_{ys}\\ D_{sx} & D_{sy} & D_{ss}\end{bmatrix}\begin{Bmatrix}\kappa_x\\ \kappa_y\\ \kappa_s\end{Bmatrix} \quad (11)$$

where N_{ij} are normal and shear forces per unit length, M_{ij} are bending and twisting moments per unit length, A_{ij} are the extensional stiffness, B_{ij} are the coupling stiffness, and D_{ij} are the bending stiffness. Also, A_{ij}, B_{ij} and D_{ij} are defined as

$$A_{ij} = \sum_{k=1}^{n} Q_{ij}^k(h_k - h_{k-1}) \quad (12)$$

$$B_{ij} = \frac{1}{2}\sum_{k=1}^{n} Q_{ij}^k(h_k^2 - h_{k-1}^2) \quad (13)$$

$$D_{ij} = \frac{1}{3}\sum_{k=1}^{n} Q_{ij}^k(h_k^3 - h_{k-1}^3) \quad (14)$$

where Q_{ij}^k are the stiffness matrix for layer k, and h_k is the distance from the neutral surface defined by the reference plane to the upper and lower surfaces of the layer k. The complete set of equations can be expressed in the matrix form as

$$\begin{Bmatrix}\boldsymbol{N}\\ \boldsymbol{M}\end{Bmatrix} = \begin{bmatrix}\boldsymbol{A} & \boldsymbol{B}\\ \boldsymbol{B} & \boldsymbol{D}\end{bmatrix}\begin{Bmatrix}\varepsilon^0\\ \kappa\end{Bmatrix} \quad (15)$$

As shown in Eq. (15), the number of nonzero terms in the laminate stiffness matrix is reduced for certain laminate configurations. Symmetry or anti-symmetry of geometric and material properties about the middle surface, ply orientation, and ply stacking sequences are the parameters that govern the form of the laminate stiffness matrix.

Depending on ply staking sequences, laminate ply angle may be symmetric and anti-symmetric with respect to the middle surface. In other words, a laminate is called symmetric when there is a corresponding layer at an equal distance from the reference plane on the other side with identical thickness, orientation, and properties for each layer on one side of a reference plane. The laminate has symmetries in the mid-plane for both geometry and material properties.

For a symmetry condition, a coupling stiffness will consist of pairs of terms of equal, absolute values and in opposite signs. Thus, B_{ij} for a symmetric laminate are 0 and no coupling exists between in-plane loading and out-of-plane deformation (curvature). On the other hand, an anti-symmetric laminate has plies of identical material and thickness at equal positive and negative distances from the middle surface based on the ply orientations which are anti-symmetric with respect to the middle surface. Thus, all the terms in the laminate stiffness matrices are nonzero.

3. Failure Analysis of Laminate

Macro-mechanical failure theories for composites have been proposed by extending and adapting isotropic failure theories. All theories can be expressed in terms of the basic strength parameters referred to the principal material axes. In this study, Tsai-Hill and Tsai-Wu failure criteria are adapted for the failure analysis of laminates. Tsai-Hill criterion has the form of

$$\frac{\sigma_1^2}{F_1^2}+\frac{\sigma_2^2}{F_2^2}+\frac{\tau_6^2}{F_6^2}-\frac{\sigma_1\sigma_2}{F_1^2} = 1 \tag{16}$$

where F_1 is longitudinal strength (tensile strength when $\sigma_1>0$ and compressive strength when $\sigma_1<0$), F_2 is transverse strength, and F_6 is in-plane shear strength. The assumption of Tsai-Hill criterion is that the tension and compression have an equal strength. In comparison, Tsai-Wu criterion is able to consider the different strengths in tension and compression in the Tsai-Wu criterion. Tsai-Wu criterion is described by the tensor polynomial as

$$f_1 = \sigma_i + f_{ij}\sigma_i\sigma_j \tag{17}$$

where the contracted notation $i, j = 1, 2, ..., 6$ is used, and f_i and f_{ij} are fexperimental strength tensors of the second and fourth ranks, respectively.

As the damage grows, the stiffness of the damaged ply as well as that of the entire laminate is reduced. As the limit state, crack density laminate modulus is reduced to approximately 90% of its original value and the in-situ modulus of the 90° layer is reduced to approximately 25% of its original value. In this study, the stiffness reduction factor of laminate of 0.25 is used based on the experimental result by Daniel and Ishai (1994). In order to obtain the stress-strain relationship of CFS for various laminated angles, it is important to find a

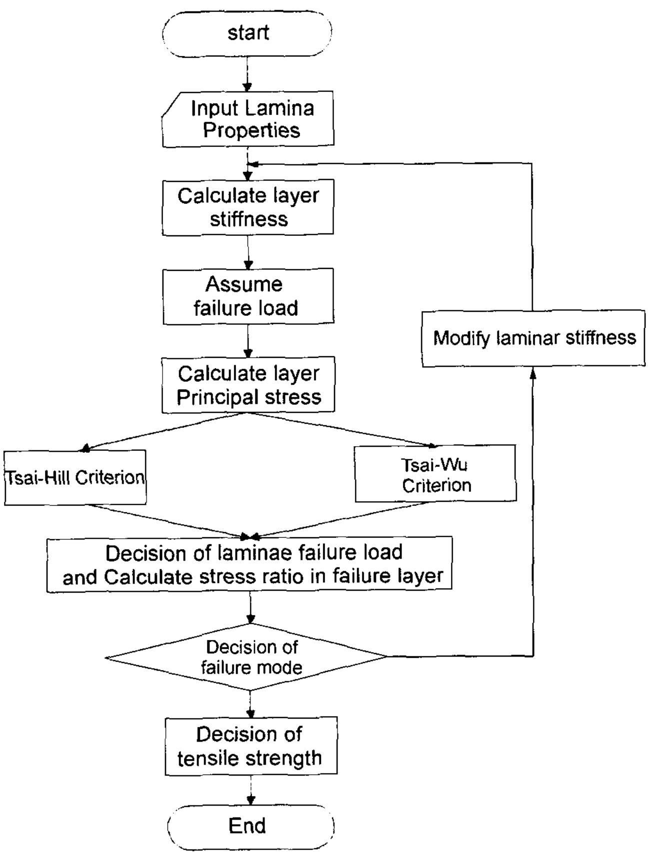

Fig. 2. Flowchart for failure analysis of laminate.

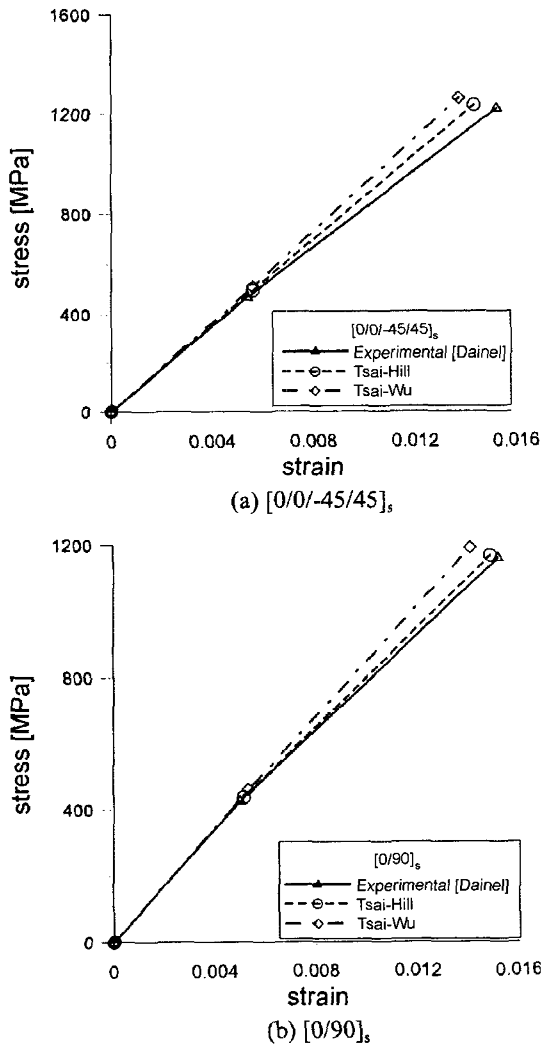

Fig. 3. Stress-strain curve of CFS laminate.

layer where first-ply-failure occurs in advance. Simultaneously, the loads and strains at the time of a failure should be determined. The stiffness of damaged ply is modified by using the reduction factor. Then, one can recalculate the stress state of each ply and investigate a new stress-distribution. The above procedures will be repeated until the next failure of lamina. Finally, when all plies reach their failure state, a stress-strain curve of carbon fiber sheets is derived. Fig. 2 shows the algorithm for analysis that obtains the stress-strain relationships of laminate.

In order to verify the developed algorithm, the results of analyses are compared with the experimental data from other studies (Fig. 3). CFS products used in this study is IM6/SC1081 and AS4/350-6 Carbon/Epoxy laminate. Experimental results and material properties are obtained from Daniels experiment (1994). Fig. 3 shows that the developed failure algorithm for laminate using both Tsai-Hill and Tsai-Wu criteria shows good agreements with Daniels experimental results.

4. Analysis on the Stress-strain Relationship of Concrete Members Confined with CFS

The stress-strain relationship of concrete members confined with CFS is obtained using two different approaches. One is the analytic model for the stress-strain relationship of the concrete member confined with CFS by Mander *et al.* (1988). The other is the empirical model for stress-strain relationship proposed by Hosotani *et al.* (1998) and Nakatsuka *et al.* (1998). Since the stress-strain relationship proposed by Mander *et al.* (1988) is obtained by modifying the results from the confinement effects of concrete members confined with hoops or spiral reinforcements, it is fundamentally not proper to represent the confinement effects of concrete members confined with CFS. Therefore, in this study, the empirical model for stress-strain relationship proposed by Hosotani *et al.* (1998) and Nakatsuka *et al.* (1998) is used to develop a confinement effect analysis algorithm. Brief reviews of Hosotani and Nakatsuka models are given in next two sections.

4.1 Hosotani model

Hosotani *et al.* (1998) proposed their model based on two-step relationships as shown in Fig. 4. More specifically, this model shown in Fig. 4 was divided into two domains according to the ratios of reinforcement. The formulae for stress-strain curves by Hosotani are tabulated in Table 1.

Here, E_g is defined according to the shape of the cross section of the compressed specimen.

$$E_g = -0.658\frac{f_{co}^2}{\rho_{cf}\varepsilon_{cft}E_{cf}} + 0.078\sqrt{\rho_{cf}}E_{cf} \quad (18)$$

(circular section)

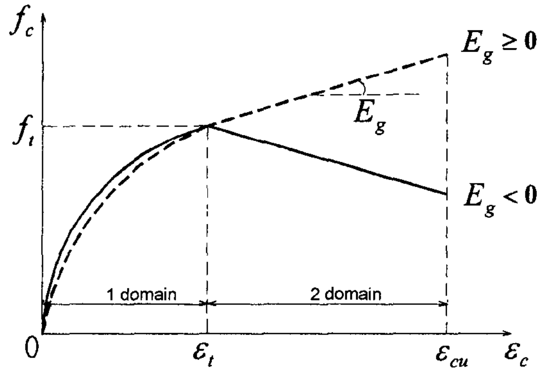

Fig. 4. Stress-strain model of Hosotani.

Table 1. The Empirical formulas of Hosotani model.

Domain	Empirical Formula	List of Symbols
$0 \leq \varepsilon_c \leq \varepsilon_t$	$f_c = E_c\varepsilon_c\left\{1-\frac{1}{n}\left(\frac{\varepsilon_c}{\varepsilon_1}\right)^{n-1}\right\}$ $(E_g<0)$ $f_c = E_c\varepsilon_c\left\{1-\frac{1}{n}\left(\frac{\varepsilon_c}{\varepsilon_1}\right)^{n-1}\right\}$ $(E_g<0)$	f_c : compressive stress of confined concrete ε_c : longitudinal compressive concrete strain f_t : compressive strength ε_t : strain at compressive strength f_t ρ_s : ratio of volume of transverse reinforcement E_c : initial Youngs modulus E_g : second domain grade value
$\varepsilon_t \leq \varepsilon_c \leq \varepsilon_{cu}$	$f_c = f_t + E_g(\varepsilon_c - \varepsilon_t)$ $n = \frac{E_c\varepsilon_t}{E_c\varepsilon_t - f_t}$ $(E_g<0)$ $n = \frac{(E_c - E_g)\varepsilon_t}{E_c\varepsilon_t - f_t}$ $(E_g<0)$	

$$E_g = -1.198\frac{f_{co}^2}{\rho_{cf}\varepsilon_{cft}E_{cf}} + 0.012\sqrt{\rho_{cf}}E_{cf} \quad (19)$$

(rectangular section)

4.2 Nakatsuka model

The model proposed by Nakatsuka *et al.* (1998) is divided into three domains as shown in Fig. 5.

The formulae for stress curves are tabulated in Table 2. As same as in Hosotani *et al.* model, the three sections are divided accordin to the ratio of reinforcements.

4.3 The calculation of ultimate compressive failure strain of confined concrete

To calculate the ultimate longitudinal compressive failure strain of confined concrete, two approaches are used. One is based on an energy balance method proposed by Scott *et al.* (1982) and the other is based on the empirical formulae developed by Hosotani *et al.* (1998). In this study, the latter is used to evaluate the ultimate compressive failure strain of concrete. The ultimate compressive failure strains suggested by Hosotani are given as follows according to the cross sectional shapes

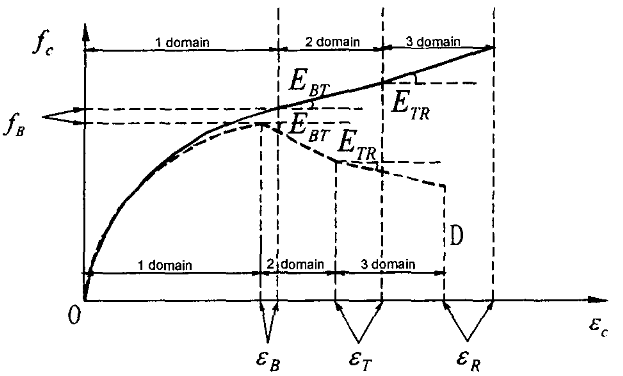

Fig. 5. Stress-strain model of Nakatsuka.

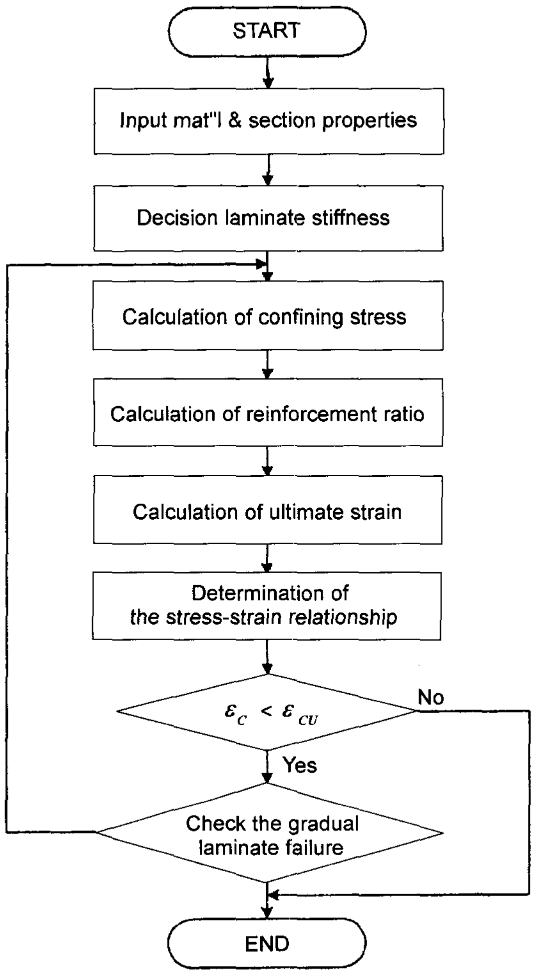

Fig. 6. Flowchart of confinement effect analysis.

Table 2. Empirical formulas of Nakatsuka model.

Domain	Empirical Formula	List of Symbols
$0 \le \varepsilon_t \le \varepsilon_B$	$f_c = E_c\varepsilon_B\left\{\frac{\varepsilon_c}{\varepsilon_B} - \frac{a}{n}\left(\frac{\varepsilon_c}{\varepsilon_B}\right)^n\right\}$ $n = \frac{E_c\varepsilon_B}{E_c\varepsilon_B - f_B} \times a, a = \begin{cases} 1 & (E_{BT} \le 0) \\ 1 - \frac{E_{BT}}{E_c} & (E_{BT} > 0) \end{cases}$	f_c : longitudinal stress E_c : first domain grade value E_{BT} : second domain grade value E_{TR} : third domain grade value f_B : compressive stress ε_B : strain at compressive stress f_B ε_T : strain at regular grade ε_R : strain at fiber failure
$\varepsilon_B < \varepsilon_c \le \varepsilon_T$	$f_c = f_B + E_{BT}\left(\frac{\varepsilon_c}{\varepsilon_B} - 1\right)$	
$\varepsilon_T < \varepsilon_c \le \varepsilon_R$	$f_c = f_B + E_{BT}\varepsilon_B\left(\frac{\varepsilon_c}{\varepsilon_B} - 1\right) + E_{TR}\varepsilon_T\left(\frac{\varepsilon_R}{\varepsilon_T} - 1\right)$	

of specimens.

In the above equations, E_{CF} is the longitudinal Youngs modulus of CFS and is the volume ratio of ρ_{CFS} defined as

$$\rho_{CF} = 4 \times N \times t_{CF}/d \tag{22}$$

where t_{CF} is the thickness of a ply, N is the number of lamination, and d is the length of the section.

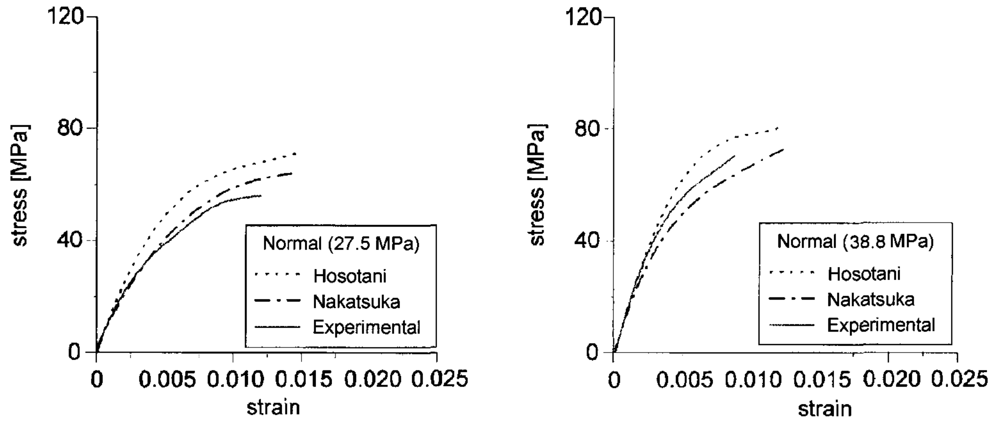

(a) Normal strength concrete (b) High strength concrete

Fig. 7. Compressive strength of concrete based confinement effects of concrete members reinforced with CFS.

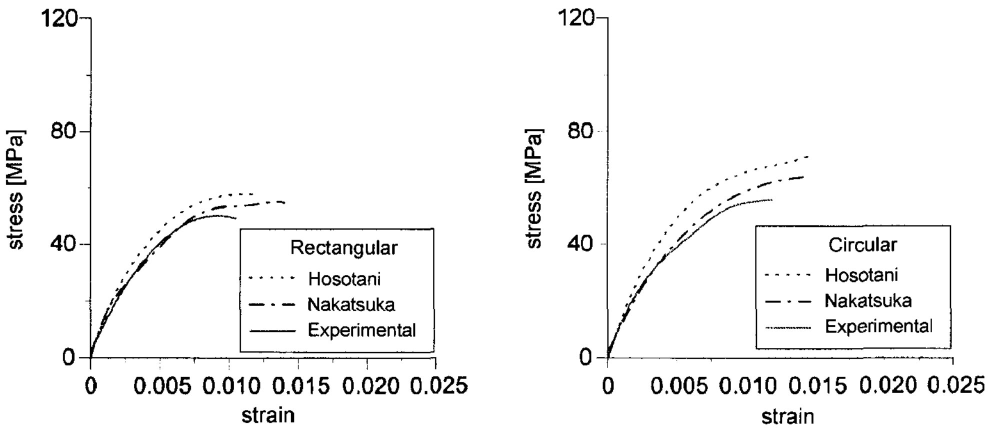

(a) Rectangular specimen (b) Circular specimen

Fig. 8. Specimen cross sectional shape based confinement effects of concrete members reinforced with CFS.

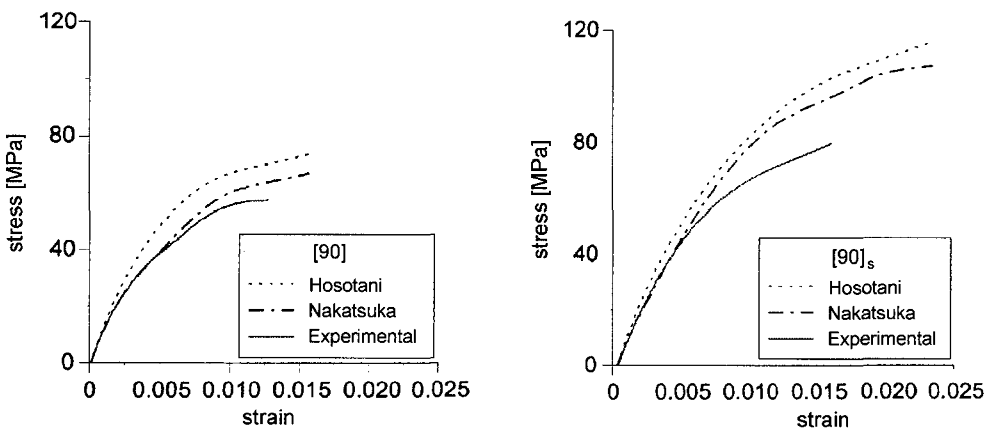

(a) 1-ply (0.45 %) (b) 2-ply (0.89 %)

Fig. 9. Reinforcement ratio based confinement effects of concrete members reinforced with CFS.

4.4 An analysis algorithm for the the confinement effect of reinforced concrete members

The stress-strain models stated in sections 4.1-4.3 are implemented and combined to develop the lamina analysis algorithm for the stress-strain relationship of concrete members as shown in Fig. 6.

Using the algorithm shown in Fig. 6, the stress-strain relationship of concrete members confined with CFS are

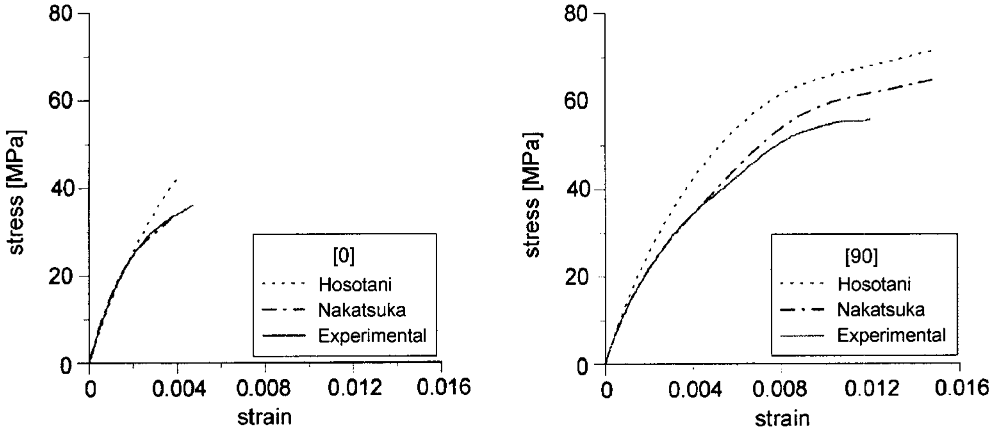

(a) Perpendicular to loading axes (b) Parallel to loading axes

Fig. 10. Lamina fiber direction based confinement effects of concrete members reinforced with CFS.

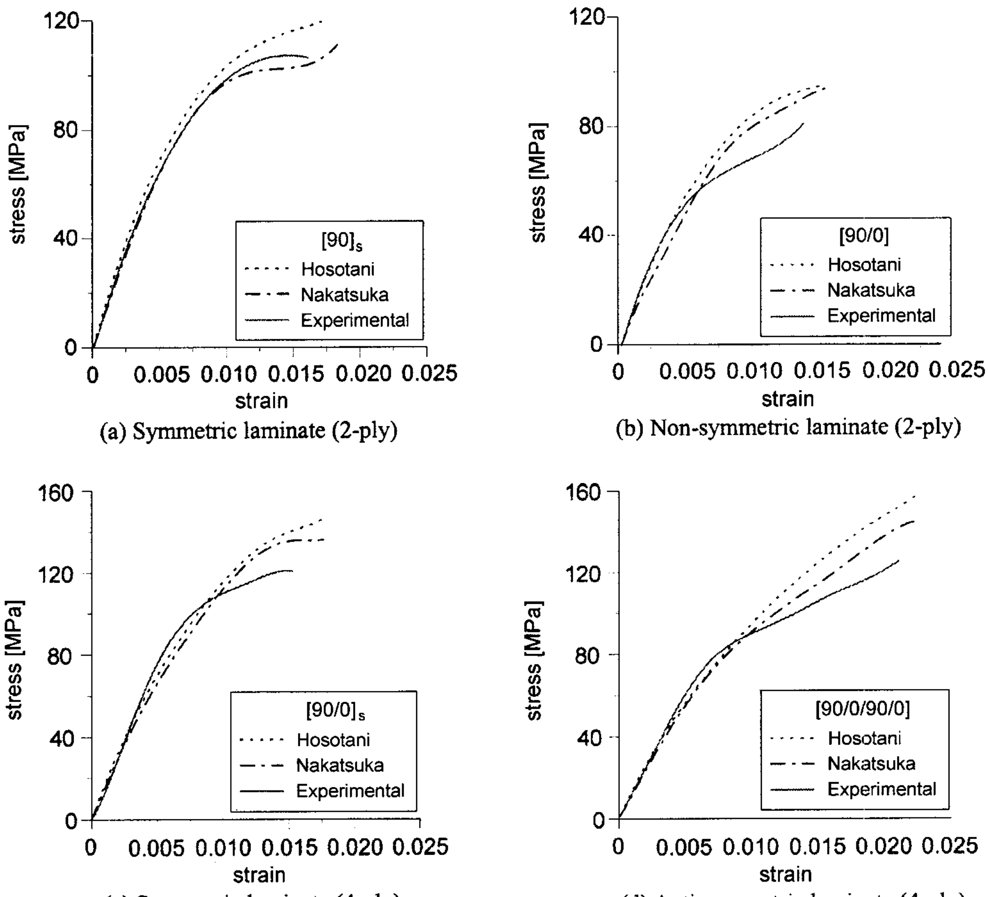

(a) Symmetric laminate (2-ply) (b) Non-symmetric laminate (2-ply)

(c) Symmetric laminate (4-ply) (d) Anti-symmetric laminate (4-ply)

Fig. 11. Stacking sequences of laminate confinement effects of concrete members reinforced with CFS.

presented according to the various parameters such as a compressive strength of unconfined concrete, a ratio of reinforcement, a cross-sectional shape of specimen, fiber direction of lamina, and stacking sequences of laminates.

The experimental data and procedures which are compared to the analytical results of this study in the following discussions are already presented by Lee *et al.* (1999). Fig. 7 to Fig. 11 show better agreements of stress-strain curves for Nakatsuka *et al.* (1998) than Hosotani *et al.* (1988) to the experimental results. It is important note that Fig. 8 shows a higher degree of confinement effect of the circular specimen than that of the rectangular specimen. In addition, Fig. 10 and Fig. 11 reveal the direct consequences of the number of laminate layers and the stacking sequences of laminates on the CFS confinement effect of concrete members. The results show that the variational fiber direction laminate stacking sequences give better confinement effect than a single fiber direction oriented laminate stacking sequences (Fig. 11). Also, a greater number of laminate plies apply higher degree of confinement stresses on the inner to concrete specimen than a fewer number of plies (Fig. 9).

5. Conclusions

In this study, the stress-strain behavior of concrete compression member confined with CFS is studied analytically. The concluding remarks are as follows

1. Using Tsai-Hill and Tsai-Wu failure criteria, the analytical stress-strain model for gradual failure of laminate for various fiber directions is developed;
2. The developed fiber composite laminate model is implemented into Nakatsuka and Hosotani stress-strain confined concrete relationships to develop a new model for the analysis of confined concrete for various fiber direction laminates;
3. Modified Nakatsuka model having the ability to consider multi-angle fiber directions of laminates better simulates the experimental results than that of the modified Hosotani model;
4. The results from the analysis of the fiber composite confined concrete using the newly developed model when compared to the experimental results for various parameters such as a core concrete compressive strengths, reinforcement ratios, specimen sectional shapes, laminate fiber directions, and laminate stacking sequences show good agreements.

Acknowledgment

This work was supported by the Brain Korea 21 Project in 2001.

References

Ahmed SH, Shah SP (1985) Behavior of hoop confined concrete under high strain rates, ACI Journal, 82(5): 634-647.

Choi SH, Kim JU, Ko YJ, Bae JS (1999) A study on the confined effect of FRP sheet reinforced concrete columns in freezing-thawing, Proceedings of Korean Society of Civil Engineers, 1: 517-520.

Daniel IM, Ishai O (1994) Engineering Mechanics of Composite Materials, Oxford University Press.

Hosotani M, Kawashima K, Hoshikuma J (1997) A study on confinement effect of concrete cylinders by carbon fiber sheets, Proceedings of the 3rd International Symposium, Non-Metallic (FRP) Reinforcement for Concrete Structure, 1: 209-216.

Hosotani M, Kawashima K, Hoshikuma J (1998) A stress-strain model for concrete cylinders confined by carbon fiber sheets, Journal of Materials, Concrete Structures and Pavement, JSCE, 39(2): 37-52 (in Japanese).

Jang IY, Lee SH, Park HG, Na HC (1999) An experimental study on the stress-strain behavior of concrete columns strengthened with carbon fiber laminate, Proceedings of Korean Concrete Institute, 11(2): 509-512.

Jeong SU, Ryu C, Kim ES, Kim WI, Kim SS (1997) A study on the enhancement of strength of laterally confined concrete by carbon-fiber sheet Proceedings of Korean Concrete Institute, 9(2): 462-471.

Kwon YW, Chung SC (1999) A study on mechanical characteristics of reinforced concrete columns confined with carbon fiber sheet, Proceedings of Korean Concrete Institute, 11(1): 743-749.

Lee HH, Koo ES (1999) An experimental study on the hysteretic capacity evaluation of the shear-strengthened RC column with carbon fiber sheet, Proceedings of Korean Concrete Institute, 11(1): 750-755.

Lee HK, Kim SC, Yoo SH, Kim JK, Chung L (1998) Estimation of confinement stress for concrete compressive member rehabilitated with carbon fiber laminate, Proceedings of Korean Concrete Institute, 10(1): 593-600.

Lee WI, Kim TU, Yoon KJ (1995) New Composite Materials, Kyo-Hak Press.

Lim GT, Chung SY (1992) A study on the behavior of the confined high-strength reinforced concrete columns, Proceedings of Korean Architecture Institute, 8(10): 163-171.

Lee SH, Jang IY, Kim HJ, Na HC (1999) Analysis of the stress-strain relationship of concrete compression member strengthened by composite materials, Proceedings of Korean Concrete Institute, 11(2): 717-720.

Malek AM, Saadatmanesh H (1998) Analytical study of reinforced concrete beams strengthened with web-bonded fiber reinforced plastic plates or fabrics, ACI Structural Journal, 95(3): 343-352.

Mander JB, Priestley MJN, Park R (1988) Theoretical stress-strain model for confined concrete, Journal of Structural Engineering, ASCE, 114(8): 1804-1826.

Nakatsuka I, Komura S, Takaki T (1998) A longitudinal stress-strain relation for confined concrete with carbon fiber sheets, JCI Structural Journal, 9(2): 65-77.

Popovics S (1973) Numerical approach to the complete stress-strain curves for concrete, Cement and Concrete Research, 3(5): 582-599.

Priestley MJN, Park R (1987) Strength and ductility of concrete bridge columns under seismic loading, ACI Structural Journal, 84(1): 61-76.

Saadatmanesh H, Ehsani MR, Li MW (1994) Strength and ductility of concrete columns externally reinforced with fiber composite straps, ACI Structural Journal, 91(4): 434-447.

Scott BD, Park R, Priestley MJN (1982) Stress-strain behavior of concrete confined by overlapping hoops at low and high strain rates, ACI Structural Journal, 79(1): 13-27.